



Diagnostic efficacy of bone scintigraphy in transthyretin cardiac amyloidosis: an updated systematic review and Bayesian bivariate meta-analysis

Dan Ruan¹ · Long Sun²

Received: 19 September 2021 / Accepted: 24 October 2021 / Published online: 12 November 2021
© Italian Association of Nuclear Medicine and Molecular Imaging 2021

Abstract

Purpose Radionuclide bone scintigraphy is increasingly attracting the attention of clinicians as a tool for the specific diagnosis of transthyretin (ATTR) cardiac amyloidosis. We aimed to describe the diagnostic value of bone scintigraphy in ATTR amyloid cardiomyopathy (ATTR-CA) by performing a meta-analysis of multiple studies.

Methods We searched all literature included in PubMed and EMBASE until August 10, 2021. A Bayesian bivariate meta-analysis was used for all included studies. Diagnostic performance of bone scan for the diagnosis of ATTR-CA was assessed by calculating pooled sensitivity, specificity, LLR + (Log positive likelihood ratio), LLR – (Log negative likelihood ratio), LDOR (Log diagnostic odds ratio), and plotting forest maps. Summary receiver operating characteristic curves (SROC) were fitted based on a Bayesian bivariate hierarchical model to assess the overall diagnostic efficacy of bone scan for the diagnosis of ATTR-CA. A meta-analysis with subgroups based on imaging time, diagnostic criteria, and different radiotracers was performed to compare the differences in diagnostic efficacy.

Results We included a total of 39 publications with a total of 3636 patients. The pooled sensitivity, specificity, LLR +, LLR –, and LDOR of bone scan for diagnosing ATTR-CA were 0.97, 0.96, 3.22, – 3.59, and 6.81, respectively; the SROC curve showed excellent diagnostic performance with an area under the curve of 0.99. The semi-quantitative visual score method, quantitative ratio (i.e., H/CL, H/WB, H/M) analysis, and quantitative cardiac SUVmax/peak analysis all had higher pooled sensitivity (0.97 vs. 0.98 vs. 1.00); the pooled specificity of cardiac SUVmax analysis was lower than that of visual scoring and quantitative ratio analysis (0.87 vs. 0.96 vs. 0.96). Regarding imaging time, the pooled sensitivity, specificity, LLR +, LLR – and LDOR were better for 3-h imaging than 1-h (0.98 vs. 0.97; 0.97 vs. 0.95; 3.49 vs. 3.03; – 3.91 vs. – 3.72; 7.40 vs. 6.75). Among the different bone-seeking tracers, the pooled sensitivities of ^{99m}Tc-DPD, ^{99m}Tc-PYP, and ^{99m}Tc-HMDP were 0.98, 0.95, and 1.00, respectively, and the pooled specificities were 0.94, 0.95, and 0.98, respectively.

Conclusions Bone scintigraphy has an excellent diagnostic performance in ATTR-CA. An accurate diagnosis of ATTR-CA can be made based on the semi-quantitative visual score, quantitative ratios of planar imaging, and cardiac bone-tracer uptake values of SPECT images.

Keywords ATTR-CA · Cardiac amyloidosis · ^{99m}Tc-DPD · ^{99m}Tc-PYP · ^{99m}Tc-HMDP

Introduction

Amyloidosis is a disease that results from the deposition of amyloid fibrils in the extracellular space, destroying the structure of tissues and consequently causing damage to multiple organ systems. The common clinical types are immunoglobulin light-chain (AL) amyloidosis and transthyretin (ATTR) amyloidosis, accounting for 59.1% and 32.9% of patients with amyloidosis. AL amyloidosis is due to excessive secretion of monoclonal light chains by bone marrow plasma cells and aggregation into amyloid fibrils deposited

✉ Long Sun
13178352662@163.com

¹ Department of Nuclear Medicine, Zhongshan Hospital, Fudan University (Xiamen Branch), Xiamen, China

² Department of Nuclear Medicine and Minnan PET Center, Xiamen Cancer Hospital, The First Affiliated Hospital of Xiamen University, 55 Zhenhai Rd., Xiamen 361003, China

in tissues, often involving the liver, lung, kidney, lower urinary tract, bone marrow, and rarely the heart [1]. ATTR amyloidosis is caused by the misfolding of transthyretin proteins, which aggregate into amyloid fibrils and accumulate in tissues, mainly involving the heart, carpal tunnel, spinal ligaments, and peripheral nerves [2–4]. When ATTR or AL amyloid is deposited in the myocardium, it causes thickening of the ventricular wall, diastolic dysfunction, restricted systolic function, impaired transmission, and ultimately heart failure. Research studies have shown that approximately 20% of heart failure and myocardial wall thickening patients have wild-type transthyretin cardiac amyloidosis [5].

In the past 20 years, cardiac amyloidosis has often been considered a rare disease and has not received much attention. Patients with early-onset ATTR-CA tend to often present with decreased exercise tolerance and slowly progressive decreased diastolic heart function, and these non-specific symptoms can mostly lead to delayed diagnosis or miss the best time for treatment. The earliest examinations to suspected heart-related discomforts are electrocardiogram (ECG) and echocardiography. ECG is performed as a routine exam. Approximately 34–46% of patients with amyloid cardiomyopathy exhibit low voltage in the limb leads, with mutant ATTR amyloid cardiomyopathy (ATTRm-CA) and wild-type ATTR amyloid cardiomyopathy (ATTRwt-CA) accounting for 38% and 18%, respectively [6, 7]. The characteristic manifestations of ATTR-CA diagnosed by echocardiography are mainly preserved ejection fraction and left ventricular hypertrophy, which is nonspecific and can also occur in hypertensive hypertrophic heart disease and hereditary hypertrophic cardiomyopathy [8]. A further examination, cardiac MRI, has good diagnostic sensitivity (95%) and specificity (98%) for amyloid cardiomyopathy but does not provide a specific differential diagnosis between ATTR-CA and other cardiomyopathies [9]. In addition, the gold standard for the diagnosis of ATTR-CA is an endomyocardial biopsy, which is invasive, risky, and needs to be performed by a physician with excellent expertise.

Current treatment modalities for ATTR-CA include chemotherapy, transthyretin protein reduction, and liver transplantation, and the prognosis after treatment is much better than that of AL amyloid cardiomyopathy (AL-CA) [10]. Therefore, early diagnosis and treatment are crucial. ^{99m}Tc-labelled bone tracer has been used for a long time for the diagnosis of ATTR-CA. The advantage of bone imaging agents is the specificity in differentiating ATTR-CA from AL-CA and other types of cardiomyopathies. Published studies in various countries have shown good diagnostic efficacy of technetium-99m diphosphono-1,2-propanodicarboxylic acid (^{99m}Tc-DPD), technetium-99m pyrophosphate (^{99m}Tc-PYP), and technetium-99m hydroxymethylene diphosphonate (^{99m}Tc-HMDP) imaging for ATTR-CA, but most studies included too few patients. In addition, the

clinical application of bone scans for the diagnosis of ATTR-CA is still in the early clinical trial stage in many countries and regions. Therefore, we included multiple studies in our meta-analysis to assess diagnostic performance from overall diagnostic efficacy to specific differential applications (different imaging time, different diagnostic criteria, different bone-seeking tracers), thus providing more comprehensive and more adequate diagnostic evidence for the use of bone scintigraphy in cardiac disease.

Materials and methods

Search strategy

This review followed the Preferred Reporting Items for a Systematic Review and Meta-Analysis (PRISMA) statement [11]. Ethical approval or informed consent was not required by conducting a meta-analysis of published studies without reference to specific patients for inclusion.

We searched the published literature by utilizing the PubMed database and EMBASE database with a search deadline of August 10, 2021. The search formula used was: (((amyloid[Title/Abstract] OR amyloidosis[Title/Abstract]) AND (TTR[Title/Abstract] OR ATTR[Title/Abstract] OR transthyretin[Title/Abstract])) AND (scintigraphy[Title/Abstract] OR scan[Title/Abstract] OR SPECT[Title/Abstract] OR SPET[Title/Abstract] OR bone[Title/Abstract] OR skeletal[Title/Abstract] OR skeleton[Title/Abstract] OR PYP[Title/Abstract] OR DPD[Title/Abstract] OR HMDP[Title/Abstract] OR MDP[Title/Abstract] OR HDP[Title/Abstract])). There was no restriction on the language of the article.

Study selection and exclusion

We included studies that met the following criteria: (1) studies in which ^{99m}Tc-PYP or ^{99m}Tc-DPD or ^{99m}Tc-HMDP imaging were used for the diagnosis of ATTR-CA; (2) diagnostically relevant data could be extracted, such as true-positive (TP), false-positive (FP), false-negative (FN), true-negative (TN), sensitivity, and specificity; (3) studies with no less than ten cases. The following types of literature were excluded: (1) non-human studies; (2) case report, review, editorial, letter, comment, conference proceedings, conference abstract, and articles without full-text.

Articles that did not meet the criteria were first excluded through the database filters, and then the remaining articles that did not meet the criteria were further excluded by carefully reading the title, abstract, and full text. Two authors decided the final included articles, and any disagreements were resolved through consensus discussions.

Data extraction and quality assessment

We extracted relevant information from the included literature, including first author, year of publication, country, study design, number of patients, age of patients, type of patients, diagnostic modality, type of imaging agent, and reference standard. TP, FP, FN, and TN were extracted directly or calculated indirectly by reading the full text. Two authors assessed the methodology of each study using the entries in the Quality Assessment of Diagnostic Accuracy Studies-2 (QUADAS-2) questionnaire [12].

Statistical analysis

First, we assessed the quality of the included studies using RevMan software (Review Manager, version 5.4). The included studies' visual assessment method, quantitative ratio (i.e., H/CL, H/WB, H/M) analysis, and myocardial SUV analysis may have used different thresholds in the diagnostic process. We used a Bayesian bivariate random-effects model analysis to fully consider the variation among studies and the correlation between pooled sensitivity and specificity. We obtained the pooled sensitivity, specificity, LLR +, LLR –, and LDOR using the “INLA” package [13] (the integrated nested Laplace approximation based on INLA to combine the data) and the “meta4diag” package [14] (the bivariate meta-analysis based on the Bayesian framework principle) in R (R for Windows, version 4.1.0). The fitted SROC curves obtained from the modelling based on the Logit transformation were used to assess the overall efficacy of bone scan for ATTR-CA diagnosis. In addition, for subgroup data with more zero values and insufficient data that could not be pooled by R software, the pooled sensitivity and specificity were calculated after correction by adding 0.5 to the cells with zero values using MetaDiSc software (Meta-analysis of Diagnostic and Screening Tests, version 1.4) [15]. Finally, publication bias was assessed by plotting funnel plots using the R package described above [16].

Results

Literatures search and study characteristics

We retrieved 383 articles on PubMed, 1021 articles on EMBASE, and two articles by manual search. First, a total of 1177 articles were excluded by the automatic filters of the database; then, 167 articles were excluded by reading the titles and abstracts of the remaining 229 articles; further, 23 articles were excluded by carefully reading the full text of the remaining 63 articles. Finally, 39 articles were included in our meta-analysis [5, 17–54]. The detailed search and selection process are shown in Fig. 1.

We included 39 studies published between 2002 and 2021, 28 retrospective and 11 prospective, with a total of 3636 patients and a mean or median age span of 54.4–86 years. There were 12 studies using ^{99m}Tc -DPD, eight using ^{99m}Tc -HDMP, 16 using ^{99m}Tc -PYP, and three using multiple bone imaging agents. Four studies were analyzed quantitatively by measuring cardiac SUVmax or SUVpeak, and the remaining 35 studies were analyzed by semi-quantitative visual score or combined H/CL (heart to contralateral chest retention) or H/WB (heart to whole-body retention) or H/M (heart to mediastinum retention) ratios. The reference standard for 28 of these studies was subendocardial biopsy or combined with extracardiac tissue biopsy; for 8 studies, the reference standard was extracardiac tissue biopsy, gene sequencing, and immunohistochemistry; and for the other 3 studies, the reference standard was typical imaging image presentation, clinical features, and immunohistochemistry. The essential characteristics of the included studies are detailed in Table 1.

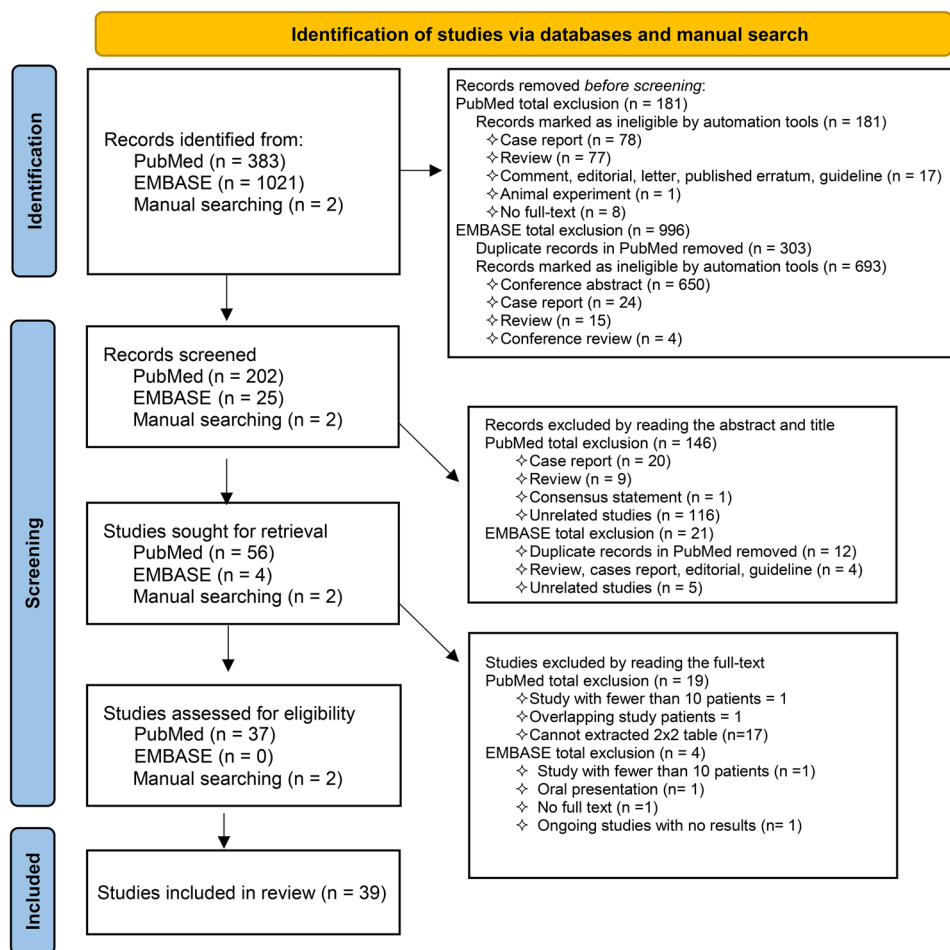
Methodological qualitative analysis

Figure 2a shows the risk bias and clinical usability issues for each included study regarding patient selection, experimental methodology, reference standard, and study flow. Figure 2b presents a summary assessment of all included studies in terms of methodology. Fourteen studies reported that they included patients on a consecutive basis [19, 23, 34, 35, 37, 39, 42–45, 51–54], and 25 studies did not report whether they were consecutive [5, 17, 18, 20–22, 24–33, 36, 38, 40, 41, 46–50]. Regarding the index test and reference standard, 16 studies were blinded [18, 19, 21–23, 28, 29, 36, 37, 40, 42, 45, 50, 51, 54], 21 did not report whether they were blinded, and two studies were unblinded [31, 47], while ten studies had a reference standard other than pathology [5, 18, 19, 34, 35, 38–41, 47], thus introducing a high risk in the index test and the reference standard. Further, Asif and Bellevre's study used the visual score of bone scintigraphy as a reference standard, leading to the concern of clinical applicability [34, 47]. Since Löfbacka's study included patients with known ATTRm-CA and positive bone scan, there is a clinical applicability concern in patient selection [49].

Overall pooled diagnostic performance of bone scintigraphy

Figure 3 shows a forest plot of the pooled sensitivity and specificity of bone scan for the diagnosis of ATTR-CA. The high pooled sensitivity (0.97, 95% CI 0.95–0.99) and specificity (0.96, 95% CI 0.94–0.98) of the 39 included studies indicate the excellent performance of bone scan for the diagnosis of ATTR. Figure 4 shows forest plots of positive likelihood ratio, negative likelihood ratio, and

Fig. 1 Flow chart of literature search using PRISMA 2020 method



diagnostic odds ratio after logit transformation. The pooled estimates of LLR +, LLR –, and LDOR were 3.22 (95% CI 2.76–3.80), – 3.59 (95% CI – 4.58 to – 2.86), and 6.81 (95% CI 5.87–7.93), respectively. Figure 5 shows the SROC curve and the estimate of AUC (0.99, 95% CI 0.95–0.99). The dark blue SROC line shown in Fig. 5 is particularly close to the upper left corner, suggesting that the diagnostic value of bone scintigraphy is exceptionally high.

Pooled diagnostic performance of each subgroup set

Table 2 shows the pooled sensitivity, specificity, LLR +, LLR –, LDOR, and 95% CI for each subgroup.

Visual scoring, quantitative ratio (i.e., H/CL, H/WB, H/M) analysis, and myocardial SUVmax/peak analysis showed high pooled sensitivities of 0.97 (95% CI 0.94–0.98), 0.98 (95% CI 0.96–1.00), and 1.00 (95% CI 0.95–1.00), respectively, for diagnosing ATTR-CA. The pooled specificities were higher for visual scoring (0.96, 95% CI 0.94–0.98) and quantitative ratio analysis (0.96, 95% CI 0.92–0.99) and lowered for myocardial SUVmax/peak

(0.87, 95% CI 0.79–0.93). The pooled LLR +, LLR – and LDOR of quantitative ratio analysis were higher than visual scoring [3.33 (95% CI 2.45–4.59) vs. 3.21 (95% CI 2.71–3.83); – 4.06 (95% CI – 5.45 to – 3.05) vs. – 3.41 (95% CI – 4.15 to – 2.80); 7.39 (95% CI 5.97–9.23) vs. 6.62 (95% CI 5.84–7.48)], indicating that quantitative ratio analysis may be superior to visual scoring in identifying ATTR-CA.

On the other hand, when the diagnostic threshold for visual scoring was score 1 (five data sets), the pooled sensitivity, specificity, LLR +, LLR –, and LDOR were 0.99 (95% CI 0.97–1.00), 0.93 (95% CI 0.78–0.99), 3.02 (95% CI 1.35–5.27), – 4.62 (95% CI – 6.33 to – 3.44), and 7.64 (95% CI 5.58–10.35), respectively. When the diagnostic threshold was score 2 (32 data sets), the pooled sensitivity, specificity, LLR +, LLR –, and LDOR 0.96 (95% CI 0.93–0.98), 0.96 (95% CI 0.94–0.98), 3.16 (95% CI 2.66–3.79), – 3.12 (95% CI – 3.91 to – 2.51), and 6.28 (95% CI 5.43–7.23), respectively.

Regarding imaging time, the pooled sensitivity, specificity, LLR +, LLR –, and LDOR for studies in which the time from radiotracer injection to scanning was 30 min–1 h

Table 1 Characteristics of included studies

Year	Author	Ref.	Origin	Study design	No. of pts.	Age (mean/median/ range)	Data-type	Index test	Time of acquiring image	Basic parameters	Reference Standard
2002	Puille M	[17]	Germany	Re	18	54.4 (ATTR)	8 ATTR, 10 other	Visual score, H/WB ratio	3 h	DPD-WB, SPET	EMB, ETB, Genotyping, IMH
2005	Perugini E	[18]	Italy	Re	35	56 (ATTR)	15 ATTR, 10 AL, 10 other	Visual score, H/WB ratio	3 h	DPD-WB, SPECT	Genotyping, IMH
2011	Rapezzi C	[19]	Italy	Re	94	62 (ATTR)	45 ATTR, 34 AL, 15 other	Visual score, H/WB ratio	3 h	DPD-WB, SPECT	Genotyping, IMH
2012	De Haro-del	[20]	Spain	Re	19	82 (ATTR)	8 ATTR, 11 AL	Visual score	3 h	DPD-WB, SPECT	EMB, ETB
2013	Bokhari S	[21]	USA	Pro	45	73 (ATTR)	33 ATTR, 12 AL	Visual score, H/CL ratio	1 h	PYP-PC, SPECT	EMB, ETB, Genotyping, IMH
2014	Hutt DF	[22]	UK	Re	321	75 (ATTR)	178 ATTR, 44 AL, 99 other	Visual score	3 h	DPD-WB, SPECT/ CT	EMB, ETB, Genotyping, IMH
2015	Galat A	[23]	France	Pro	98	64–87 (ATTR)	47 ATTR, 14 AL, 37 other	Visual score	3 h	HMDP-WB	EMB, ETB, Genotyping, IMH
2015	Papantoniou V	[24]	Greece	Re	12	69 (all patients)	6 ATTR, 6 AL	Visual score, H/CL ratio	1, 2 and 3 h	PYP-PC, SPET	EMB, IMH
2016	Castano A	[25]	USA	Re	171	75 (ATTR)	121 ATTR, 34 AL, 16 other	Visual score, H/CL ratio	1 and 3 h	PYP-PC	EMB, Genotyping, IMH
2016	Grillmore JD	[26]	Several	Re	374	NR	261 ATTR, 62 AL, 51 other	Visual score	1 and 3 h	DPD/HMDP-WB, PYP-PC	EMB, ETB, Genotyping, IMH
2017	Cappelli F	[27]	Italy	Re	85	78.7 (ATTR)	39 ATTR, 26 AL, 20 other	Visual score, H/WB ratio	150 min	HMDP-WB	EMB, ETB, Genotyping, IMH
2017	Cariou E	[28]	France	Pro	50	72 (all patients)	31 ATTR, 18 AL, 1 other	Visual score, H/WB ratio	3 h	HMDP-WB	EMB, ETB, Genotyping, IMH
2017	Moore PT	[29]	Australia	Pro	21	70 (ATTR)	13 ATTR, 8 AL	Visual score	3 h	DPD-WB, SPECT/ CT	EMB, Genotyping
2018	Daquarti GJ	[30]	Argentina	Re	46	84 (ATTR)	26 ATTR, 5 AL, 1 other	Visual score, H/CL ratio	1 h	PYP-PC or HMDP-PC	EMB, ETB, Genotyping, IMH
2018	Ramsay SC	[31]	Australia	Pro	29	76.5 (ATTR)	6 ATTR, 1 AL, 22 other	Visual score, Cardiac SUVmax	3 h	HMDP-WB, xSPECT	EMB, ETB, IMH
2019	Kircher M	[32]	Germany	Re	16	75 (ATTR)	5 ATTR, 7 AL, 4 other	Visual score	3 h	DPD-WB	EMB, ETB, IMH
2019	Tsutsui Y	[33]	Japan	Re	29	74.6 (ATTR)	9 ATTR, 20 other	Visual score, H/CL ratio	2.5 h	PYP-PC, SPECT	EMB, Genotyping, IMH
2020	Belleve D	[34]	France	Re	30	86 (ATTR)	15 ATTR, 15 other	Cardiac SUVmax	167 min	HMDP CTZ-SPECT/CT	PYP visual score, CIF, IMH
2020	Caobelli F	[35]	Switzerland	Re	13	77 (ATTR)	8 ATTR, 5 other	Cardiac SUVmax/ SUVpeak	3.5–4 h	PYP-WB, xSPECT/ CT	CIF, IMH
2020	Flaherty KR	[36]	USA	Pro	43	78 (ATTR)	24 ATTR, 3 AL, 16 other	Visual score, H/CL ratio	1 h	PYP-PC	EMB, Genotyping
2020	Maika N	[37]	France	Re	308	79 (ATTR)	182 ATTR, 65 AL, 61 other	Visual score, H/M ratio	10 and 30 min	HMDP-WB, SPECT/CT	EMB, ETB, Genotyping, IMH

Table 1 (continued)

Year	Author	Ref.	Origin	Study design	No. of pts.	Age (mean/median/range)	Data-type	Index test	Time of acquiring image	Basic parameters	Reference Standard
2020	Masri A	[38]	USA	Pro	233	77 (all patients)	60 ATTR, 173 other	Visual score, H/CL ratio	1 and 3 h	PYP-PC, SPECT	Genotyping, IMH
2020	Musumeci MB	[39]	Italy	Re	19	64 (ATTR)	19 ATTR	Visual score	5 min and 3 h	DPD/HMDP-WB	Genotyping
2020	Santarelli MF	[40]	Italy	Re	38	81 (ATTR)	18 ATTR, 20 other	Visual score	Dynamic, 1, 2 and 3 h	HMDP-D-S	Genotyping, IMH
2020	Scully PR	[41]	UK	Re	100	84 (all patients)	50 ATTR, 3 AL, 47 other	Visual score, H/CL ratio, cardiac SUV _{peak}	3 h	DPD-WB, SPECT/CT	Genotyping, IMH
2020	Singh V	[42]	USA	Re	27	NR	13 ATTR, 7 AL, 7 other	Visual score	1, 2, 3 and 5 h	PYP-PC, SPECT/CT	EMB, Genotyping
2020	Takasone K	[43]	Japan	Pro	47	57 (ATTR)	30 ATTR, 17 AL	Visual score	3.5 h	PYP-PC, SPECT	EMB, ETB, Genotyping, IMH
2020	Tamarappoo B	[44]	USA	Re	112	77 (ATTR)	39 ATTR, 26 AL, 47 other	Visual score	4 h	PYP/Tl-201 SPECT	EMB, Genotyping, IMH
2020	Usuku H	[45]	Japan	Re	109	<70 (all patients)	19 ATTR, 90 other	Visual score, H/CL ratio	3 h	PYP-PC, SPECT	EMB, ETB, IMH
2020	Zhang LX	[46]	Canada	Pro	17	79 (ATTR)	12 ATTR, 5 other	Visual score	1 and 3 h	PYP-PC, SPECT/CT	EMB, ETB, Genotyping, IMH
2021	Asif T	[47]	USA	Re	133	76 (all patients)	35 ATTR, 98 other	Visual score, H/CL ratio	1 h	PYP-PC, SPECT	Myocardial PYP uptake, IMH
2021	Gallini C ^a	[48]	Italy	Re	76	78 (ATTR)	53 ATTR, 12 AL, 11 other	Visual score, H/CL, H/WB ratio	3 h	HMDP-WB	EMB, ETB, Genotyping, IMH
2021	Lindmark K	[5]	Sweden	Re	86	NR	14 ATTR, 72 other	Visual score	NR	DPD-WB	Genotyping, IMH
2021	Löfbacka V	[49]	Sweden	Re	48	69 (ATTR)	48 ATTR	Visual score	3 h	DPD-WB, SPECT/CT	ETB, Genotyping
2021	Miller RH	[50]	Canada	Re	124	79.3 (ATTR)	43 ATTR, 81 other	Visual score	1 and 3 h	PYP-PC, SPECT	EMB, ETB
2021	Nitsche C	[51]	UK/Austria	Pro	407	83.4 (all patients)	47 ATTR, 3 AL, 357 other	Visual score	3 h	DPD-WB, SPECT	EMB, ETB, Genotyping, IMH
2021	Poterucha TJ	[52]	USA	Re	103	72.9 (ATTR)	69 ATTR, 12 AL, 22 other	Visual score	1 h	PYP-PC, SPECT	EMB, IMH
2021	Ren C	[53]	China	Pro	37	58 (ATTR)	6 ATTR, 10 AL, 21 other	Visual score, H/CL ratio	1 h	PYP-PC, SPECT/CT	EMB, ETB, Genotyping, IMH
2021	Schatka I	[54]	Germany	Re	63	77 (all patients)	25 ATTR, 5 AL, 33 other	Visual score, H/CL ratio	1 and 3 h	DPD-PC, SPECT	EMB, ETB

Ref reference; No. of pts number of patients; DPD-WB ^{99m}Tc-DPD Whole-body (WB) Planar scintigraphy; PYP-WB ^{99m}Tc-PYP WB Planar scintigraphy; PYP-PC ^{99m}Tc-PYP planar cardiac scintigraphy; HMDP-WB ^{99m}Tc-HMDP WB Planar scintigraphy; HMDP-D-S ^{99m}Tc-HMDP Dynamic and static planar cardiac scintigraphy; DPD-PC ^{99m}Tc-DPD planar cardiac scintigraphy; PYP/Tl-201 SPECT ^{99m}Tc-PYP and ²⁰¹Tl SPECT myocardial imaging; xSPECT xSPECT/CT QUANT; EMB endomyocardial biopsy; ETB extracardiac biopsy; IMH immunohistochemistry; CIF conventional imaging findings

^aGallini C's study had a replication of 26 patients (4 ATTRwt, 6 ATTRmt, 5 AL, and 11 other) with Cappelli F

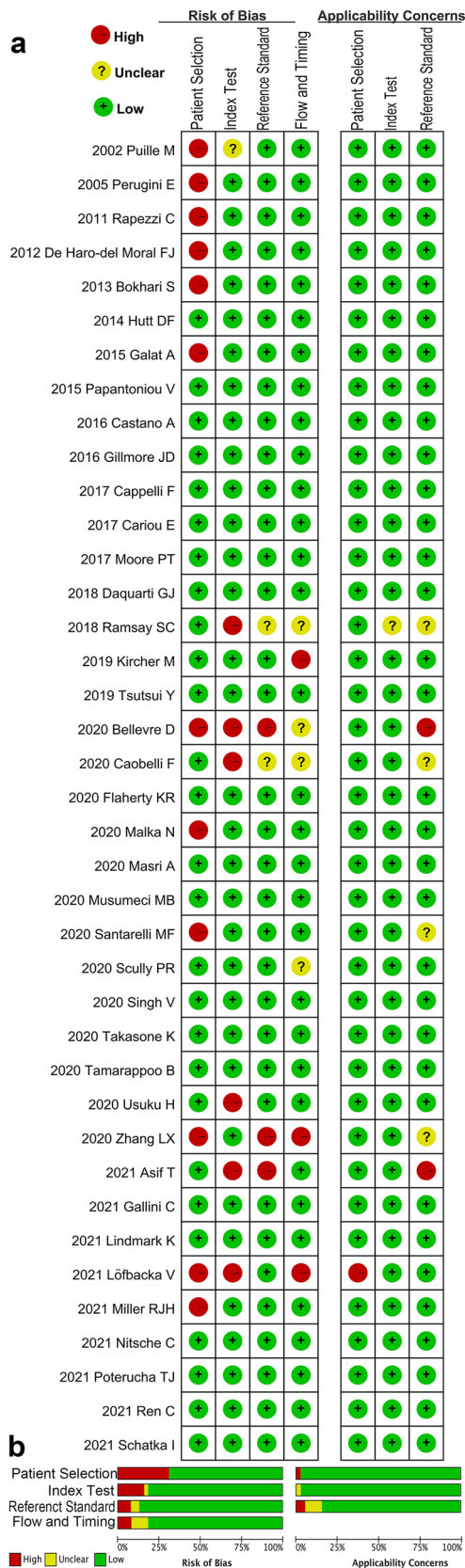


Fig. 2 Quality evaluation of the methodology of each included study and overall assessment of risk bias and applicability concerns for included studies based on the QUADAS-2 method

(14 data sets) were 0.97 (95% CI 0.95–0.99), 0.95 (95% CI 0.93–0.97), 3.03 (95% CI 2.68–3.49), – 3.72 (95% CI – 4.90 to – 2.08), and 6.75 (95% CI 5.68–8.04), respectively. The pooled sensitivity, specificity, LLR +, LLR –, and LDOR for studies in which the imaging time was 2.5–4 h after radiotracer injection (33 data sets) were 0.98 (95% CI 0.95–0.99), 0.97 (95% CI 0.94–0.99), 3.49 (95% CI 2.82–4.35), – 3.91 (95% CI – 5.22 to – 2.97), and 7.40 (95% CI 6.27–8.79), respectively. Overall, pooled sensitivity, specificity, LLR +, LLR – and LDOR were higher at an imaging time of approximately 3 h than at approximately 1 h.

When grouped according to the type of imaging agent, the pooled sensitivity, specificity, LLR +, LLR –, and LDOR for imaging with ^{99m}Tc-DPD (12 data sets) were 0.98 (95% CI 0.96–1.00), 0.94 (95% CI 0.88–0.98), 2.82 (95% CI 2.06–3.79), – 4.52 (95% CI – 7.55 to – 3.03), and 7.34 (95% CI 5.47–10.47), respectively. The pooled sensitivity, specificity, LLR +, LLR –, and LDOR for imaging with ^{99m}Tc-PYP (16 data sets) were 0.95 (95% CI 0.90–0.98), 0.95 (95% CI 0.93–0.97), 3.02 (95% CI 2.53–3.71), – 2.96 (95% CI – 4.07 to – 2.16), and 5.98 (95% CI 4.94–7.35), respectively. The pooled sensitivity, specificity, LLR +, LLR –, and LDOR for imaging with ^{99m}Tc-HMDP (9 data sets) were 1.00 (95% CI 0.98–1.00), 0.98 (95% CI 0.96–1.00), 4.24 (95% CI 3.07–6.27), – 6.38 (95% CI – 11.72 to – 3.80), and 10.62 (95% CI 7.63–15.55), respectively.

Publication bias

By visual analysis of the funnel plot (Fig. 6), we found eight studies scattered outside the 95% confidence interval of the funnel plot, indicating heterogeneity among our included studies. In addition, a large number of studies were distributed at the bottom of the funnel plot, indicating that we included a large number of small sample studies. Observing the studies within the 95% confidence interval as a whole, we found that these studies were roughly symmetrically distributed on both sides of the LDOR estimates, thus indicating that there was no significant publication bias in the inclusion of our meta-analysis.

Discussion

Bone-seeking radiopharmaceuticals have been used for the diagnosis of ATTR-CA for 20 years. Most clinical studies based on the diagnosis of ATTR-CA have a small number of cases due to the limited therapeutic effect of amyloid cardiomyopathy and the lack of awareness of the disease among clinicians. The previous meta-analysis has shown good diagnostic performance with bone scans [55]. Our study is a Bayesian bivariate meta-analysis based on a

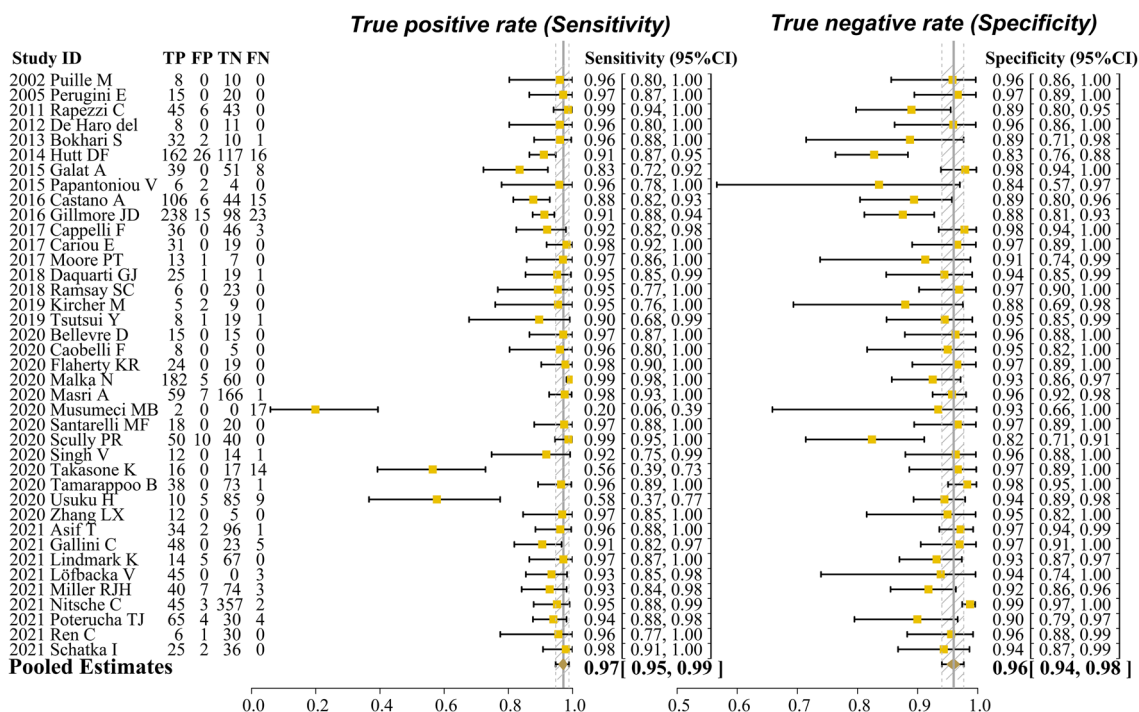


Fig. 3 Forest plot for the pooled sensitivity (true positive rate) and specificity (true negative rate)

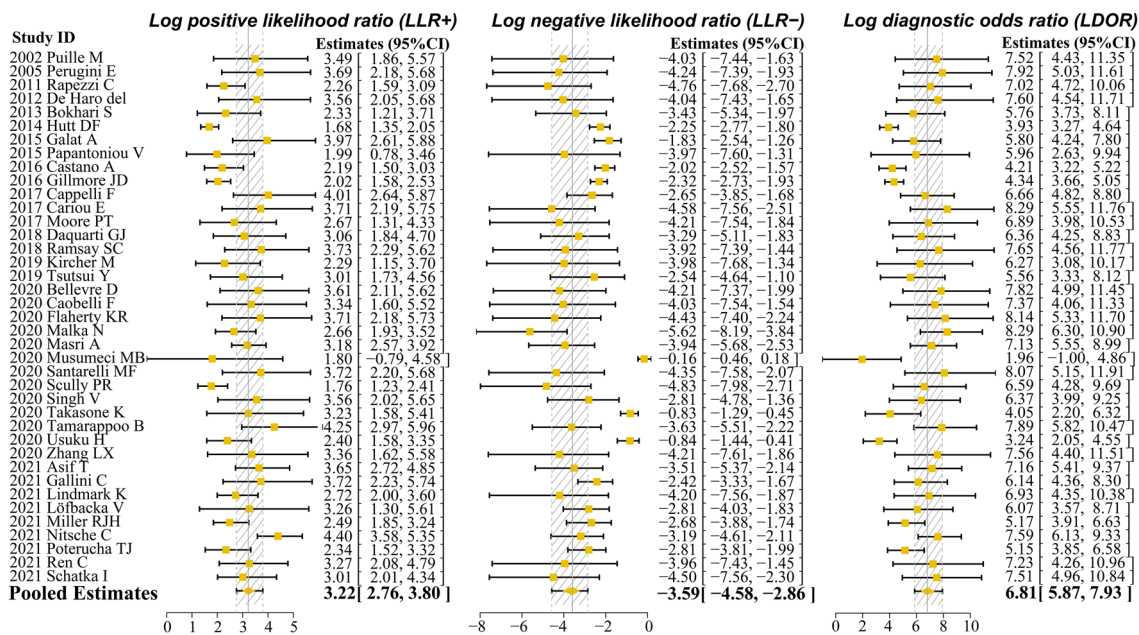


Fig. 4 Forest plot for the pooled LLR -, LLR+, and LDOR

previous study by adding many new publications. In addition, a meticulous subgroup meta-analysis was performed to assess the difference in diagnostic efficacy of bone scintigraphy for ATTR-CA.

Electrocardiography and echocardiography are the most common examinations for patients with suspect amyloid cardiomyopathy or other cardiac diseases. Low voltage in the limb leads of the ECG combined with septal thickening

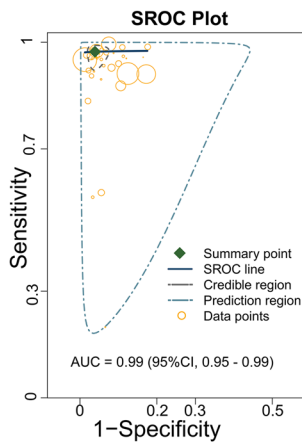


Fig. 5 SROC curve for the evaluation of the overall performance of bone scan for the diagnosis of ATTR-CA

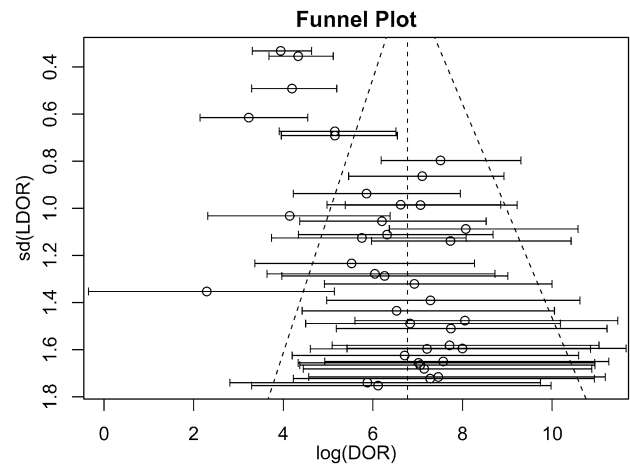


Fig. 6 Funnel plot on bone scintigraphy for the diagnosis of ATTR-CA

(> 12 mm) on echocardiography can distinguish ATTR-CA from other diseases associated with septal thickening with a sensitivity and specificity of 100% and 95%, respectively

[56, 57]. However, only 25% of patients with ATTR-CA showed low voltage in the limb leads, and the lack of

Table 2 Comparison of diagnostic performance between subgroups

Data-type	Pooled sensitivity (95% CI)	Pooled specificity (95% CI)	Pooled LLR + (95% CI)	Pooled LLR - (95% CI)	Pooled LDOR (95% CI)
Time of acquiring image					
About 1-h ^a	0.97 (0.95, 0.99)	0.95 (0.93, 0.97)	3.03 (2.68, 3.49)	- 3.72 (- 4.90, - 2.08)	6.75 (5.68, 8.04)
About 3-h ^b	0.98 (0.95, 0.99)	0.97 (0.94, 0.99)	3.49 (2.82, 4.35)	- 3.91 (- 5.22, - 2.97)	7.40 (6.27, 8.79)
Diagnostic method					
Visual score	0.97 (0.94, 0.98)	0.96 (0.94, 0.98)	3.21 (2.71, 3.83)	- 3.41 (- 4.15, - 2.80)	6.62 (5.84, 7.48)
H/CL or H/WB or H/M	0.98 (0.96, 1.00)	0.96 (0.92, 0.99)	3.33 (2.45, 4.59)	- 4.06 (- 5.45, - 3.05)	7.39 (5.97, 9.23)
^c Cardiac SUVmax or SUVpeak	1.00 (0.95–1.00)	0.87 (0.79–0.93)	NA	NA	NA
Visual score cut-off					
Score 1	0.99 (0.97, 1.00)	0.93 (0.78, 0.99)	3.02 (1.35, 5.27)	- 4.62 (- 6.33, - 3.44)	7.64 (5.58, 10.35)
Score 2	0.96 (0.93, 0.98)	0.96 (0.94, 0.98)	3.16 (2.66, 3.79)	- 3.12 (- 3.91, - 2.51)	6.28 (5.43, 7.23)
Radiotracer type					
^{99m} Tc-DPD	0.98 (0.96, 1.00)	0.94 (0.88, 0.98)	2.82 (2.06, 3.79)	- 4.52 (- 7.55, - 3.03)	7.34 (5.47, 10.47)
^{99m} Tc-PYP	0.95 (0.90, 0.98)	0.95 (0.93, 0.97)	3.02 (2.53, 3.71)	- 2.96 (- 4.07, - 2.16)	5.98 (4.94, 7.35)
^{99m} Tc-HMDP	1.00 (0.98, 1.00)	0.98 (0.96, 1.00)	4.24 (3.07, 6.27)	- 6.38 (- 11.72, - 3.80)	10.62 (7.63, 15.55)

NA not available

^aAbout 1-h, imaging time from 30 min to 1 h

^bAbout 3-h, imaging time from 2.5 to 4 h

^cCardiac SUVmax or SUVpeak does not have enough data sets to calculate its pooled LLR -, LLR +, and LDOR

specificity in the presentation of septal thickening made it difficult to differentiate between ATTR-CA and AL-CA in clinical practice [58]. A meta-analysis study showed that late gadolinium enhancement cardiovascular MRI has a high diagnostic value in diagnosing amyloid cardiomyopathy, with a sensitivity and specificity of 85% (95% CI 77–91%) and 92% (95% CI 83–97%), respectively, but fails to diagnose ATTR-CA subtype and AL-CA subtype specifically [59]. Our meta-analysis showed that bone scan had excellent diagnostic efficacy for ATTR-CA, with sensitivity, specificity, and AUC of 0.97, 0.96 and, 0.99, respectively.

First, it is noteworthy that the results of our analysis suggest better diagnostic performance with 3-h imaging compared to 1 h, which is consistent with the findings of previous studies. Singh et al. found that the concentration of bone-seeking tracer in the cardiac cavity blood pool was still higher at 1 hour after the radiopharmaceutical injection and therefore delayed imaging to 3 h [42]. Masri's study also demonstrated that increased blood pool activity affects visual diagnostic results. In his study, images with an imaging time of 1 h and 3 h were scored differently in nine patients according to visual scoring criteria (i.e., nine false positives appeared in 1-h imaging). Therefore, 1-h imaging is recommended to be combined with SPECT/CT imaging to accurately differentiate between myocardial tracer uptake and ventricular blood pool tracer aggregation to reduce false positives [38].

Second, the predominant method for diagnosing ATTR-CA is the Perugini grading system, a semi-quantitative visual analysis method [18]. Our results suggest that the diagnostic efficacy of the visual scoring method is comparable to that of the quantitative ratio (H/CL or H/WB, or H/M) analysis methods. It has been shown that there is no difference in diagnostic accuracy between the visual scoring method and the quantitative ratio method, and both methods can be well mastered and applied by experienced readers and novices [42]. In a retrospective study, the Perugini visual score (≥ 2) of planar imaging had a better diagnostic performance for ATTR-CA and was almost comparable to ^{99m}Tc -PYP SPECT imaging. In contrast, the planar image's H/CL ratio (≥ 1.5) performed poorly as a diagnostic criterion, with a sensitivity and specificity of 0.57 and 0.95, respectively [47]. It is noteworthy that the diagnostic criterion based on the visual score of planar images alone is flawed. In the study of Poterucha, 32% of patients with positive visual assessment results were due to excessive tracer accumulation in the cardiac blood pool [52]. This increased uptake of cardiac blood pool leading to decreased visual diagnostic accuracy is widespread. Therefore, in most studies, patients with a visual score of 1 or 2 on planar imaging underwent further SPECT imaging [19, 21, 22, 29, 38, 42, 51]. In addition, it has been shown that the visual judgment method of SPECT images alone has higher diagnostic sensitivity (1.00

vs. 0.93) and specificity (0.99 vs. 0.91) than the visual grading score of planar images [50]. Therefore, routinely adding SPECT or SPECT/CT imaging to improve the diagnostic accuracy of ATTR-CA should become a routine procedure [47, 60]. Another noteworthy aspect is that some researchers have concluded that the diagnostic performance of absolute quantitative measurements of myocardial radiotracer uptake values and visual grading score are in good agreement. In all of these studies, the sensitivity of myocardial SUVmax/peak for diagnosing ATTR-CA reached 100%. Moreover, the quantitative myocardial uptake values from SPECT/CT also more accurately reflect the load of myocardial amyloid deposition [31, 34, 35, 41, 61]. This finding may also herald the potential value of SPECT/CT quantitative myocardial radiotracer uptake values in diagnosis, efficacy assessment of treatment, and prognosis prediction that can be explored.

Furthermore, the results of our meta-analysis showed that the diagnostic threshold of the visual score of 1 was more sensitive but less specific than that of 2. The studies of Gillmore and Cappelli compared the diagnostic performance of a visual score of 1 and a visual score of 2 and found that score 1 was more sensitive and less specific than score 2 [26, 27]. AL-CA was a frequent cause of false positives and was predominantly distributed in the group with a visual score of 1. Quarta et al. mentioned that 39% of AL-CA patients had varying degrees of ^{99m}Tc -DPD uptake. Moreover, patients with AL-CA presenting with ^{99m}Tc -DPD uptake tend to have a poorer cardiac function and a worse prognosis, so care should be taken to distinguish ATTR-CA from AL-CA at the time of diagnosis carefully [62]. In addition to AL-CA, the presence of the following disorders can also lead to the false-positive diagnosis, including extensive myocardial infarction, unstable angina, cardiotoxicity due to adriamycin, pericarditis, alcoholic cardiomyopathy, pericardial tumors, and hypercalcemia [63].

It has been shown that ^{99m}Tc -MDP, the radiotracer most commonly used for bone scintigraphy, is less concentrated in the myocardium of ATTR-CA patients and is less suitable as a specific cardiac imaging agent for the diagnosis of ATTR-CA [18, 20]. The imaging agents routinely used for the diagnosis of ATTR-CA are ^{99m}Tc -DPD, ^{99m}Tc -PYP, and ^{99m}Tc -HMDP. All three tracers are effective for the diagnosis of ATTR-CA. Studies have demonstrated differences in pharmacokinetics, plasma protein binding, renal excretion, and degree of bone binding between ^{99m}Tc -DPD and ^{99m}Tc -HMDP, but the differences in uptake and distribution in patients with ATTR-CA have not been conclusively established [64–66]. The results of our meta-analysis showed differences in pooled sensitivity and specificity between the different imaging agents, which may also suggest slight differences in the affinity of bone-seeking tracers for ATTR amyloid-deposited myocardium. In a comparative study of dual nuclide imaging in six patients, the author described

a mild difference in the degree of concentration of ^{99m}Tc -HMDP and ^{99m}Tc -DPD in the myocardium of ATTR-CA patients, but the difference was not statistically significant [67]. Unfortunately, few studies have directly compared the differences of these three imaging agents in diagnosing ATTR-CA. In clinical practice, most hospitals choose bone-seeking radiopharmaceuticals for cardiac use not based on better diagnostic performance, no doubt, but rather on which imaging agent is more readily available.

ATTR-CA is divided into ATTRwt-CA (senile systemic amyloidosis) and ATTRm-CA (familial amyloid cardiomyopathy). Studies on the diagnosis of ATTRwt-CA have shown that bone scintigraphy has superior diagnostic sensitivity and specificity [5, 51]. Similarly, bone scintigraphy has excellent diagnostic accuracy in patients with amyloid cardiomyopathy with common mutant TTR genotypes. However, bone scintigraphy is not ideal for the diagnosis of amyloid cardiomyopathy with rare TTR genotypes. In Musumeci's study, the sensitivity (10.5%) and diagnostic accuracy (37%) of bone scintigraphy were very low for ATTR-CA with Phe64Leu TTR gene mutation [39]. Other researchers have similarly found low myocardial uptake of the bone radiotracer in ATTR-CA patients with Phe64Leu mutation, leading to false-negative results [52]. Thus, the original mechanisms of bone tracer binding to ATTR amyloid-deposited myocardium, including high calcium loading in ATTR amyloid tissue leading to the high uptake of bone radiotracer and high affinity of ATTR amyloid fibrous tissue for bone radiotracer leading to the high uptake of the bone radiotracer, remain to be further investigated.

Another aspect that deserves our attention is the current development of SPECT instruments and application software, especially the highly sensitive 360-degree rotating cadmium telluride (CZT) detector, which improves the diagnostic accuracy of nuclear medicine. Compared to the conventional sodium iodide (NaI) detector, the CZT detector offers higher detection efficiency and better detection sensitivity, i.e., reducing the dose of tracer used and reducing the imaging duration while ensuring better image clarity. The efficacy of the SPECT gamma camera equipped with the CTZ detector for diagnosing ATTR-CA performed better in all the studies we included, with a diagnostic sensitivity of almost 100% [34, 36, 44, 54].

Finally, we need to mention some limitations in this meta-analysis. First, our inclusion criteria were not very strict, and the most important of which needs to be discussed is that not all the reference standards of our included literature were endocardial biopsies. Some studies used tissue biopsies of carpal tunnel ligaments and spinal ligaments as the reference standard for diagnosis. Eldhagen et al. found that the presence of ATTR amyloid deposition in the ligamentum flavum of the patient with lumbar spinal stenosis was not associated with ATTR amyloid deposits in the myocardium

[68]. By analyzing surgical resection specimens, Sueyoshi found that patients with bilateral carpal tunnel syndrome had a 33.3% incidence of ATTR amyloid deposition in carpal tunnel ligaments or tendons, and patients with lumbar spinal stenosis had a 44.4% incidence of ATTR amyloid deposition in spinal ligaments [69]. It has also been shown that patients with ATTR mutations have an 87.5% positive rate of amyloid detection by Congo-red staining of the carpal tunnel ligament [70]. Therefore, the diagnostic accuracy calculated based on reference standards of biopsies of non-cardiac tissue for diagnosing ATTR-CA by bone scan may deviate to some extent from the actual accuracy. There are also studies in which the reference standard included biopsies of abdominal adipose tissue. Studies that included a large number of amyloidosis cases have found that abdominal fat pad aspiration biopsy has a low diagnostic sensitivity for ATTR amyloidosis (12–27.3%) but a relatively high diagnostic sensitivity for AL amyloidosis (73.2–84%) [71–73]. Thus, abdominal fat biopsy as a diagnostic method to exclude AL is safe, applicable, and relatively accurate. Further, we included several studies for specific patient populations, including Musumeci's study of patients with the Phe64Leu genotype, a rare type of TTR mutation [39], Nitsche's study of patients with cardiomyopathy with aortic stenosis [51], and Lindmark's study of patients with ATTRwt-CA only [5]. It could be partly responsible for the heterogeneity between studies. Finally, we included many studies with small samples, which may indicate the low stability of the results of our meta-analysis.

Conclusions

Bone-seeking tracers (^{99m}Tc -DPD, ^{99m}Tc -PYP, and ^{99m}Tc -HMDP) play an essential role in diagnosing ATTR-CA. One hour and 3-h imaging images show differences in the degree of radiotracer concentration in the ventricular blood pool, resulting in slight differences in diagnostic sensitivity and specificity. The visual evaluation of planar cardiac imaging is sufficient to make an accurate diagnosis of ATTR-CA, but the combination of SPECT imaging significantly improves the specificity and sensitivity of the diagnosis. Both quantitative ratios (H/CL, H/WB, H/M) from planar imaging and quantitative cardiac bone tracer uptake values from quantitative SPECT imaging provide accurate diagnostic information. However, bone scans are not very effective in diagnosing ATTR-CA patients with rare mutation types.

Author contributions LS provided the ideas for this review, and DR completed the analysis of the data and the writing of the manuscript. The search and inclusion of the literature were done by both authors.

Funding No funding was received to assist with the preparation of this manuscript.

Data availability All analytical data are included in this article. If the original data tables are required, they can be obtained by contacting the corresponding author.

Code availability When we use the R language, we use the related code of the INLA package and the meta4diag package. Detailed code is available by contacting the corresponding author.

Declarations

Conflicts of interest The authors have no conflicts of interest to declare relevant to this article's content.

Ethical approval Not applicable.

Consent to participate Not applicable.

Consent for publication Not applicable.

References

- Abe R, Katoh N, Takahashi Y, Takasone K, Yoshinaga T, Yazaki M et al (2021) Distribution of amyloidosis subtypes based on tissue biopsy site—consecutive analysis of 729 patients at a single amyloidosis center in Japan. *Pathol Int* 71:70–79. <https://doi.org/10.1111/pin.13041>
- Nakagawa M, Sekijima Y, Yazaki M, Tojo K, Yoshinaga T, Doden T et al (2016) Carpal tunnel syndrome: a common initial symptom of systemic wild-type ATTR (ATTRwt) amyloidosis. *Amyloid* 23:58–63. <https://doi.org/10.3109/13506129.2015.1135792>
- Westermarck P, Westermarck GT, Suhr OB, Berg S (2014) Transthyretin-derived amyloidosis: probably a common cause of lumbar spinal stenosis. *Ups J Med Sci* 119:223–228. <https://doi.org/10.3109/03009734.2014.895786>
- Sekijima Y, Ueda M, Koike H, Misawa S, Ishii T, Ando Y (2018) Diagnosis and management of transthyretin familial amyloid polyneuropathy in Japan: red-flag symptom clusters and treatment algorithm. *Orphanet J Rare Dis* 13:6. <https://doi.org/10.1186/s13023-017-0726-x>
- Lindmark K, Pilebro B, Sundstrom T, Lindqvist P (2021) Prevalence of wild type transthyretin cardiac amyloidosis in a heart failure clinic. *ESC Heart Fail* 8:745–749. <https://doi.org/10.1002/ehf2.13110>
- Cyrille NB, Goldsmith J, Alvarez J, Maurer MS (2014) Prevalence and prognostic significance of low QRS voltage among the three main types of cardiac amyloidosis. *Am J Cardiol* 114:1089–1093. <https://doi.org/10.1016/j.amjcard.2014.07.026>
- Murtagh B, Hammill SC, Gertz MA, Kyle RA, Tajik AJ, Grogan M (2005) Electrocardiographic findings in primary systemic amyloidosis and biopsy-proven cardiac involvement. *Am J Cardiol* 95:535–537. <https://doi.org/10.1016/j.amjcard.2004.10.028>
- Cappelli F, Baldasseroni S, Bergesio F, Perlini S, Salinaro F, Padelletti L et al (2015) Echocardiographic and biohumoral characteristics in patients with AL and TTR amyloidosis at diagnosis. *Clin Cardiol* 38:69–75. <https://doi.org/10.1002/clc.22353>
- Chatzantonis G, Bietenbeck M, Elsanhoury A, Tschöpe C, Pieske B, Tauscher G et al (2021) Diagnostic value of cardiovascular magnetic resonance in comparison to endomyocardial biopsy in cardiac amyloidosis: a multi-centre study. *Clin Res Cardiol* 110:555–568. <https://doi.org/10.1007/s00392-020-01771-1>
- Rubin J, Maurer MS (2020) Cardiac amyloidosis: overlooked, underappreciated, and treatable. *Annu Rev Med* 71:203–219. <https://doi.org/10.1146/annurev-med-052918-020140>
- Page MJ, McKenzie JE, Bossuyt PM, Boutron I, Hoffmann TC, Mulrow CD et al (2021) The PRISMA 2020 statement: an updated guideline for reporting systematic reviews. *BMJ* 372:n71. <https://doi.org/10.1136/bmj.n71>
- Whiting PF, Rutjes AW, Westwood ME, Mallett S, Deeks JJ, Reitsma JB et al (2011) QUADAS-2: a revised tool for the quality assessment of diagnostic accuracy studies. *Ann Intern Med* 155:529–536. <https://doi.org/10.7326/0003-4819-155-8-201110180-00009>
- Rue H, Martino S, Chopin N (2009) Approximate Bayesian inference for latent Gaussian models by using integrated nested Laplace approximations. *J R Stat Soc Ser B* 71:319–392
- Guo J, Riebler A (2018) meta4diag: Bayesian bivariate meta-analysis of diagnostic test studies for routine practice. *J Stat Softw* 83:1–31. <https://doi.org/10.18637/jss.v083.i01>
- Zamora J, Abaira V, Muriel A, Khan K, Coomarasamy A (2006) Meta-DiSc: a software for meta-analysis of test accuracy data. *BMC Med Res Methodol* 6:31. <https://doi.org/10.1186/1471-2288-6-31>
- Song F, Khan KS, Dinnes J, Sutton AJ (2002) Asymmetric funnel plots and publication bias in meta-analyses of diagnostic accuracy. *Int J Epidemiol* 31:88–95. <https://doi.org/10.1093/ije/31.1.88>
- Puille M, Altland K, Linke RP, Steen-Muller MK, Kiett R, Steiner D et al (2002) 99mTc-DPD scintigraphy in transthyretin-related familial amyloidotic polyneuropathy. *Eur J Nucl Med Mol Imaging* 29:376–379. <https://doi.org/10.1007/s00259-001-0730-0>
- Perugini E, Guidalotti PL, Salvi F, Cooke RM, Pettinato C, Riva L et al (2005) Noninvasive etiologic diagnosis of cardiac amyloidosis using 99mTc-3,3-diphosphono-1,2-propanodicarboxylic acid scintigraphy. *J Am Coll Cardiol* 46:1076–1084. <https://doi.org/10.1016/j.jacc.2005.05.073>
- Rapezzi C, Quarta CC, Guidalotti PL, Longhi S, Pettinato C, Leone O et al (2011) Usefulness and limitations of 99mTc-3,3-diphosphono-1,2-propanodicarboxylic acid scintigraphy in the aetiological diagnosis of amyloidotic cardiomyopathy. *Eur J Nucl Med Mol Imaging* 38:470–478. <https://doi.org/10.1007/s00259-010-1642-7>
- de Haro-del Moral FJ, Sanchez-Lajusticia A, Gomez-Bueno M, Garcia-Pavia P, Salas-Anton C, Segovia-Cubero J (2012) Role of cardiac scintigraphy with (99m)Tc-DPD in the differentiation of cardiac amyloidosis subtype. *Rev Esp Cardiol* 65:440–446. <https://doi.org/10.1016/j.recresp.2011.12.015>
- Bokhari S, Castano A, Pozniakoff T, Deslisle S, Latif F, Maurer MS (2013) (99m)Tc-pyrophosphate scintigraphy for differentiating light-chain cardiac amyloidosis from the transthyretin-related familial and senile cardiac amyloidoses. *Circ Cardiovasc Imaging* 6:195–201. <https://doi.org/10.1161/CIRCIMAGING.112.000132>
- Hutt DF, Quigley AM, Page J, Hall ML, Burniston M, Gopaul D et al (2014) Utility and limitations of 3,3-diphosphono-1,2-propanodicarboxylic acid scintigraphy in systemic amyloidosis. *Eur Heart J Cardiovasc Imaging* 15:1289–1298. <https://doi.org/10.1093/ehjci/jeu107>
- Galat A, Rosso J, Guellich A, Van Der Gucht A, Rappeneau S, Bodez D et al (2015) Usefulness of (99m)Tc-HMDP scintigraphy for the etiologic diagnosis and prognosis of cardiac amyloidosis. *Amyloid* 22:210–220. <https://doi.org/10.3109/13506129.2015.1072089>
- Papantoniou V, Valsamaki P, Kastritis S, Tsiouris S, Delichas Z, Papantoniou Y et al (2015) Imaging of cardiac amyloidosis by (99m)Tc-PYP scintigraphy. *Hell J Nucl Med* 18(Suppl 1):42–50

25. Castano A, Haq M, Narotsky DL, Goldsmith J, Weinberg RL, Morgenstern R et al (2016) Multicenter study of planar technetium 99m pyrophosphate cardiac imaging: predicting survival for patients with ATTR cardiac amyloidosis. *JAMA Cardiol* 1:880–889. <https://doi.org/10.1001/jamacardio.2016.2839>
26. Gillmore JD, Maurer MS, Falk RH, Merlini G, Damy T, Dispenzieri A et al (2016) Nonbiopsy diagnosis of cardiac transthyretin amyloidosis. *Circulation* 133:2404–2412. <https://doi.org/10.1161/CIRCULATIONAHA.116.021612>
27. Cappelli F, Gallini C, Di Mario C, Costanzo EN, Vaggelli L, Tutino F et al (2017) Accuracy of 99mTc-hydroxymethylene diphosphonate scintigraphy for diagnosis of transthyretin cardiac amyloidosis. *J Nucl Cardiol* 26:497–504. <https://doi.org/10.1007/s12350-017-0922-z>
28. Cariou E, Bennani Smires Y, Victor G, Robin G, Ribes D, Pascal P et al (2017) Diagnostic score for the detection of cardiac amyloidosis in patients with left ventricular hypertrophy and impact on prognosis. *Amyloid* 24:101–109. <https://doi.org/10.1080/13506129.2017.1333956>
29. Moore PT, Burrage MK, Mackenzie E, Law WP, Korczyk D, Mollee P (2017) The utility of (99m)Tc-DPD scintigraphy in the diagnosis of cardiac amyloidosis: an Australian experience. *Heart Lung Circ* 26:1183–1190. <https://doi.org/10.1016/j.hlc.2016.12.017>
30. Daquarti GJ, Meretta A, Corneli M, Costabel JP, Diez M, Masoli OH (2018) Bone seeking tracers' scintigraphy for the diagnosis of transthyretin cardiac amyloidosis. *Medicina* 78:395–398
31. Ramsay SC, Lindsay K, Fong W, Patford S, Younger J, Atherton J (2018) Tc-HDP quantitative SPECT/CT in transthyretin cardiac amyloid and the development of a reference interval for myocardial uptake in the non-affected population. *Eur J Hybrid Imaging* 2:17. <https://doi.org/10.1186/s41824-018-0035-1>
32. Kircher M, Ihne S, Brumberg J, Morbach C, Knop S, Kortum KM et al (2019) Detection of cardiac amyloidosis with (18) F-Florbetaben-PET/CT in comparison to echocardiography, cardiac MRI and DPD-scintigraphy. *Eur J Nucl Med Mol Imaging* 46:1407–1416. <https://doi.org/10.1007/s00259-019-04290-y>
33. Tsutsui Y, Kubota T, Kato S, Nozoe M, Suematsu N, Okabe M et al (2019) Utility of (99m)Tc-pyrophosphate scintigraphy in diagnosing transthyretin cardiac amyloidosis in real-world practice. *Circ Rep* 1:277–285. <https://doi.org/10.1253/circrep.CR-19-0015>
34. Bellevre D, Bailliez A, Delelis F, Blaire T, Agostini D, Mouquet F et al (2020) Quantitation of myocardial (99m)Tc-HMDP uptake with new SPECT/CT cadmium zinc telluride (CZT) camera in patients with transthyretin-related cardiac amyloidosis: ready for clinical use? *J Nucl Cardiol*. <https://doi.org/10.1007/s12350-020-02274-2>
35. Caobelli F, Braun M, Haaf P, Wild D, Zellweger MJ (2020) Quantitative (99m)Tc-DPD SPECT/CT in patients with suspected ATTR cardiac amyloidosis: feasibility and correlation with visual scores. *J Nucl Cardiol* 27:1456–1463. <https://doi.org/10.1007/s12350-019-01893-8>
36. Flaherty KR, Morgenstern R, Pozniakoff T, DeLuca A, Castano A, Maurer MS et al (2020) (99m)technetium pyrophosphate scintigraphy with cadmium zinc telluride cameras is a highly sensitive and specific imaging modality to diagnose transthyretin cardiac amyloidosis. *J Nucl Cardiol* 27:371–380. <https://doi.org/10.1007/s12350-019-01831-8>
37. Malka N, Abulizi M, Kharoubi M, Oghina S, Galat A, Le Bras F et al (2020) Extracardiac soft tissue uptake, evidenced on early (99m)Tc-HMDP SPECT/CT, helps typing cardiac amyloidosis and demonstrates high prognostic value. *Eur J Nucl Med Mol Imaging* 47:2396–2406. <https://doi.org/10.1007/s00259-020-04753-7>
38. Masri A, Bukhari S, Ahmad S, Nieves R, Eisele YS, Follansbee W et al (2020) Efficient 1-hour technetium-99m pyrophosphate imaging protocol for the diagnosis of transthyretin cardiac amyloidosis. *Circ Cardiovasc Imaging* 13:e010249. <https://doi.org/10.1161/CIRCIMAGING.119.010249>
39. Musumeci MB, Cappelli F, Russo D, Tini G, Canepa M, Milandri A et al (2020) Low sensitivity of bone scintigraphy in detecting Phe64Leu mutation-related transthyretin cardiac amyloidosis. *JACC Cardiovasc Imaging* 13:1314–1321. <https://doi.org/10.1016/j.jcmg.2019.10.015>
40. Santarelli MF, Genovesi D, Positano V, Di Sarlo R, Scipioni M, Giorgetti A et al (2020) Cardiac amyloidosis detection by early bisphosphonate (99mTc-HMDP) scintigraphy. *J Nucl Cardiol*. <https://doi.org/10.1007/s12350-020-02239-5>
41. Scully PR, Morris E, Patel KP, Treibel TA, Burniston M, Klotz E et al (2020) DPD quantification in cardiac amyloidosis: a novel imaging biomarker. *JACC Cardiovasc Imaging* 13:1353–1363. <https://doi.org/10.1016/j.jcmg.2020.03.020>
42. Singh V, Cuddy S, Kijewski MF, Park MA, Taylor A, Taqueti VR et al (2020) Inter-observer reproducibility and intra-observer repeatability in (99m)Tc-pyrophosphate scan interpretation for diagnosis of transthyretin cardiac amyloidosis. *J Nucl Cardiol*. <https://doi.org/10.1007/s12350-020-02353-4>
43. Takasone K, Katoh N, Takahashi Y, Abe R, Ezawa N, Yoshinaga T et al (2020) Non-invasive detection and differentiation of cardiac amyloidosis using (99m)Tc-pyrophosphate scintigraphy and (11) C-Pittsburgh compound B PET imaging. *Amyloid* 27:266–274. <https://doi.org/10.1080/13506129.2020.1798223>
44. Tamarappoo B, Otaki Y, Manabe O, Hyun M, Cantu S, Arnsorn Y et al (2020) Simultaneous Tc-99m PYP/Tl-201 dual-isotope SPECT myocardial imaging in patients with suspected cardiac amyloidosis. *J Nucl Cardiol* 27:28–37. <https://doi.org/10.1007/s12350-019-01753-5>
45. Usuku H, Takashio S, Yamamoto E, Kinoshita Y, Nishi M, Oike F et al (2020) Usefulness of relative apical longitudinal strain index to predict positive (99m) Tc-labeled pyrophosphate scintigraphy findings in advanced-age patients with suspected transthyretin amyloid cardiomyopathy. *Echocardiography* 37:1774–1783. <https://doi.org/10.1111/echo.14892>
46. Zhang LX, Martineau P, Finnerty V, Giraldeau G, Parent MC, Harel F et al (2020) Comparison of 18F-sodium fluoride positron emission tomography imaging and 99mTc-pyrophosphate in cardiac amyloidosis. *J Nucl Cardiol*. <https://doi.org/10.1007/s12350-020-02425-5>
47. Asif T, Gomez J, Singh V, Doukky R, Nedeltcheva A, Malhotra S (2021) Comparison of planar with tomographic pyrophosphate scintigraphy for transthyretin cardiac amyloidosis: perils and pitfalls. *J Nucl Cardiol* 28:104–111. <https://doi.org/10.1007/s12350-020-02328-5>
48. Gallini C, Tutino F, Martone R, Ciaccio A, Costanzo EN, Taborchi G et al (2021) Semi-quantitative indices of cardiac uptake in patients with suspected cardiac amyloidosis undergoing 99mTc-HMDP scintigraphy. *J Nucl Cardiol* 28:90–99. <https://doi.org/10.1007/s12350-019-01643-w>
49. Lofbacka V, Axelsson J, Pilebro B, Suhr OB, Lindqvist P, Sundstrom T (2021) Cardiac transthyretin amyloidosis (99m)Tc-DPD SPECT correlates with strain echocardiography and biomarkers. *Eur J Nucl Med Mol Imaging* 48:1822–1832. <https://doi.org/10.1007/s00259-020-05144-8>
50. Miller RJH, Cadet S, Mah D, Pournazari P, Chan D, Fine NM et al (2021) Diagnostic and prognostic value of technetium-99m pyrophosphate uptake quantitation for transthyretin cardiac amyloidosis. *J Nucl Cardiol*. <https://doi.org/10.1007/s12350-021-02563-4>
51. Nitsche C, Scully PR, Patel KP, Kammerlander AA, Koschutnik M, Dona C et al (2021) Prevalence and outcomes of concomitant

- aortic stenosis and cardiac amyloidosis. *J Am Coll Cardiol* 77:128–139. <https://doi.org/10.1016/j.jacc.2020.11.006>
52. Poterucha TJ, Elias P, Bokhari S, Einstein AJ, DeLuca A, Kinkhabwala M et al (2021) Diagnosing transthyretin cardiac amyloidosis by technetium Tc 99m pyrophosphate: a test in evolution. *JACC Cardiovasc Imaging* 14:1221–1231. <https://doi.org/10.1016/j.jcmg.2020.08.027>
 53. Ren C, Ren J, Tian Z, Du Y, Hao Z, Zhang Z et al (2021) Assessment of cardiac amyloidosis with (99m)Tc-pyrophosphate (PYP) quantitative SPECT. *EJNMMI Phys* 8:3. <https://doi.org/10.1186/s40658-020-00342-7>
 54. Schatka I, Bingel A, Schau F, Bluemel S, Messroghli DR, Frumkin D et al (2021) An optimized imaging protocol for [(99m)Tc] Tc-DPD scintigraphy and SPECT/CT quantification in cardiac transthyretin (ATTR) amyloidosis. *J Nucl Cardiol*. <https://doi.org/10.1007/s12350-021-02715-6>
 55. Treglia G, Glaudemans A, Bertagna F, Hazenberg BPC, Erba PA, Giubbini R et al (2018) Diagnostic accuracy of bone scintigraphy in the assessment of cardiac transthyretin-related amyloidosis: a bivariate meta-analysis. *Eur J Nucl Med Mol Imaging* 45:1945–1955. <https://doi.org/10.1007/s00259-018-4013-4>
 56. Lofbacka V, Suhr OB, Pilebro B, Wixner J, Sundstrom T, Lindmark K et al (2021) Combining ECG and echocardiography to identify transthyretin cardiac amyloidosis in heart failure. *Clin Physiol Funct Imaging* 41:408–416. <https://doi.org/10.1111/cpf.12715>
 57. Syed IS, Glockner JF, Feng D, Araoz PA, Martinez MW, Edwards WD et al (2010) Role of cardiac magnetic resonance imaging in the detection of cardiac amyloidosis. *JACC Cardiovasc Imaging* 3:155–164. <https://doi.org/10.1016/j.jcmg.2009.09.023>
 58. Rapezzi C, Merlini G, Quarta CC, Riva L, Longhi S, Leone O et al (2009) Systemic cardiac amyloidosis: disease profiles and clinical courses of the 3 main types. *Circulation* 120:1203–1212. <https://doi.org/10.1161/CIRCULATIONAHA.108.843334>
 59. Zhao L, Tian Z, Fang Q (2016) Diagnostic accuracy of cardiovascular magnetic resonance for patients with suspected cardiac amyloidosis: a systematic review and meta-analysis. *BMC Cardiovasc Disord* 16:129. <https://doi.org/10.1186/s12872-016-0311-6>
 60. Regis C, Harel F, Martineau P, Gregoire J, Abikhzer G, Juneau D et al (2020) Tc-99m-pyrophosphate scintigraphy for the diagnosis of ATTR cardiac amyloidosis: comparison of quantitative and semi-quantitative approaches. *J Nucl Cardiol* 27:1808–1815. <https://doi.org/10.1007/s12350-020-02205-1>
 61. Dorbala S, Park MA, Cuddy S, Singh V, Sullivan K, Kim S et al (2021) Absolute quantitation of cardiac (99m)Tc-pyrophosphate using cadmium-zinc-telluride-based SPECT/CT. *J Nucl Med* 62:716–722. <https://doi.org/10.2967/jnumed.120.247312>
 62. Quarta CC, Zheng J, Hutt D, Grigore SF, Manwani R, Sachithanatham S et al (2021) 99mTc-DPD scintigraphy in immunoglobulin light chain (AL) cardiac amyloidosis. *Eur Heart J Cardiovasc Imaging*. <https://doi.org/10.1093/ehjci/jeab095>
 63. Gnanasegaran G, Cook G, Adamson K, Fogelman I (2009) Patterns, variants, artifacts, and pitfalls in conventional radionuclide bone imaging and SPECT/CT. *Semin Nucl Med* 39:380–395. <https://doi.org/10.1053/j.semnuclmed.2009.07.003>
 64. Bironi FE, Persico MG, Lodola L, Concardi M, Aprile C (2015) In vitro study: binding of Tc-DPD to synthetic amyloid fibrils. *Curr Issues Pharm Med Sci* 28:231–235. <https://doi.org/10.1515/cipms-2015-0077>
 65. Jovanovic V, Maksin T, Rastovac M, Bzenic J (1983) Comparative quality control of 99mTc-pyrophosphate and 99mTc-diphosphate radiopharmaceuticals. *Eur J Nucl Med* 8:179–182. <https://doi.org/10.1007/BF00252891>
 66. McAfee JG, Krauss DJ, Subramanian G, Thomas FD, Roskopf M, Ritter C et al (1983) Comparison of 99mTc phosphate and diphosphate complexes in experimental renal infarcts. *Invest Radiol* 18:479–484. <https://doi.org/10.1097/00004424-198309000-00014>
 67. Abulizi M, Cottureau AS, Guellich A, Vandeventer S, Galat A, Van Der Gucht A et al (2018) Early-phase myocardial uptake intensity of (99m)Tc-HMDP vs (99m)Tc-DPD in patients with hereditary transthyretin-related cardiac amyloidosis. *J Nucl Cardiol* 25:217–222. <https://doi.org/10.1007/s12350-016-0707-9>
 68. Eldhagen P, Berg S, Lund LH, Sorensson P, Suhr OB, Westermark P (2021) Transthyretin amyloid deposits in lumbar spinal stenosis and assessment of signs of systemic amyloidosis. *J Intern Med* 289:895–905. <https://doi.org/10.1111/joim.13222>
 69. Sueyoshi T, Ueda M, Jono H, Irie H, Sei A, Ide J et al (2011) Wild-type transthyretin-derived amyloidosis in various ligaments and tendons. *Hum Pathol* 42:1259–1264. <https://doi.org/10.1016/j.humpath.2010.11.017>
 70. Samoes R, Taipa R, Valdez K, Goncalves I, Melo Pires M, da Silva MA et al (2017) Amyloid detection in the transverse carpal ligament of patients with hereditary ATTR V30M amyloidosis and carpal tunnel syndrome. *Amyloid* 24:73–77. <https://doi.org/10.1080/13506129.2017.1313222>
 71. Ansari-Lari MA, Ali SZ (2004) Fine-needle aspiration of abdominal fat pad for amyloid detection: a clinically useful test? *Diagn Cytopathol* 30:178–181. <https://doi.org/10.1002/dc.10370>
 72. Garcia Y, Collins AB, Stone JR (2018) Abdominal fat pad excisional biopsy for the diagnosis and typing of systemic amyloidosis. *Hum Pathol* 72:71–79. <https://doi.org/10.1016/j.humpath.2017.11.001>
 73. Quarta CC, Gonzalez-Lopez E, Gilbertson JA, Botcher N, Rowzenio D, Petrie A et al (2017) Diagnostic sensitivity of abdominal fat aspiration in cardiac amyloidosis. *Eur Heart J* 38:1905–1908. <https://doi.org/10.1093/eurheartj/ehx047>

Publisher's Note Springer Nature remains neutral with regard to jurisdictional claims in published maps and institutional affiliations.